Research Papers

Acoustic Estimation of Resonance Frequency and Sonodestruction of SonoVue Microbubbles

Rytis JURKONIS[(1)], Nerijus LAMANAUSKAS[(2)], Saulius ŠATKAUSKAS[(2)]

[(1)] *Biomedical Engineering Institute*
Kaunas University of Technology
Barsausko 59-455A, LT-51423, Kaunas, Lithuania; e-mail: rytis.jurkonis@ktu.lt

[(2)] *Biophysical Research Group*
Vytautas Magnus University
Vileikos 8, Kaunas LT-44404, Lithuania, e-mail: {n.lamanauskas, s.satkauskas}@gmf.vdu.lt

Acoustic properties of ultrasound (US) contrast agent microbubbles (MB) highly influence sonoporation efficiency and intracellular drug and gene delivery. In this study we propose an acoustic method to monitor passive and excited MBs in a real time. MB monitoring system consisted of two separate transducers. The first transducer delivered over an interval of 1 s US pulses (1 MHz, 1% duty cycle, 100 Hz repetition frequency) with stepwise increased peak negative pressure (PNP), while the second one continuously monitored acoustic response of SonoVue MBs. Pulse echo signals were processed according to the substitution method to calculate attenuation coefficient spectra and loss of amplitude. During US exposure at 50–100 kPa PNP we observed a temporal increase in loss of amplitude which coincided with the US delivery. Transient increase in loss of amplitude vanished at higher PNP values. At higher PNP values loss of amplitude decreased during the US exposure indicating MB sonodestruction. Analysis of transient attenuation spectra revealed that attenuation coefficient was maximal at 1.5 MHz frequency which is consistent with resonance frequency of SonoVue MB. The method allows evaluation of the of resonance frequency of MB, onset and kinetics of MB sonodestruction.

Keywords: SonoVue, microbubble, loss of amplitude, attenuation coefficient, resonance frequency, sonodestruction.

1. Introduction

Microbubbles (MBs) are an important tool for diagnostic image enhancement and sonoporation. Ultrasound (US) energy propagating through MBs suspension is scattered and absorbed, which results in the attenuation of echo reflected from reference reflector (GOERTZ *et al.*, 2007; ESCOFFRE et al., 2013). Recent studies have shown that both cell viability and cell transfection efficiency can be related with spectral properties of attenuation (ESCOFFRE *et al.*, 2013). This shows that detailed characterization of spectral properties of MB suspension can be an important tool in planning experimental protocols for optimal sonoporation outcomes. Indeed, several studies demonstrated that attenuation is dependent on peak negative pressure (PNP) (CHEN *et al.*, 2002; TANG *et al.*, 2005; EMMER *et al.*, 2009), which is consistent with simulations. BURNS and BECHER (2000) showed that at low PNP the echo from MB is proportional to transmitted US signal, while at larger PNP values the echo exhibits some additional frequency components. These additional frequency components are usually whole or fractional multiples (harmonics) of the excitation US frequency (TANG *et al.*, 2011). It was also shown that attenuation depends on excitation US frequency (GOERTZ *et al.*, 2007; EMMER *et al.*, 2009; TANG, ECKERSLEY, 2007; and SARKAR *et al.*, 2005). However, in most cases attenuation coefficient dependence on PNP and frequency was done in separate experiments. Experimental evaluation of both factors could reveal new features of attenuation coefficient in suspension of excited MB. Moreover, above-mentioned studies were performed at a fixed instance of time (LAMANAUSKAS *et al.*, 2013), thus neglecting transient temporal changes of attenuation coefficient. In this

study we propose an acoustic method for monitoring acoustic response of MB suspension with two separate US generators and two transducers, both working simultaneously: one for MB excitation and another for monitoring of MB acoustic response. The US excitation was delivered in small increasing steps and covered a wide range of PNP values, which allowed us to observe a transient phenomenon of MB excitation and sonodestruction occurring only at certain PNP values.

2. Materials and methods

2.1. Microbubble production

The SonoVue (Bracco, Milan, Italy) MBs were employed in the study. The experiments with MB suspension were performed within two days. For overnight storage of MBs they were kept in a refrigerator. The MB concentration was determined with the light microscope (Motic BA400, Xiamen, China). The MB concentration used in the experiments was 1×10^6 MB/ml.

2.2. US exposure and MB monitoring procedure

Two separate US systems and two transducers were used. US system to measure US echo signals was elaborated according to (ESCOFFRE *et al.*, 2013) emphasizing analysis of attenuation coefficient in time. For US exposure, we used 1 MHz sinusoidal ultrasound signal with 1% duty cycle, 100 Hz repetition frequency and exposure duration of 1 s, generated by computerised pulser from JSC Medelkom (Lithuania). The beam width of the excitation transducer was evaluated from acoustic pressure distribution scanned with hydrophone at 10 mm distance from the transducer face. The half-maximum width was found to be 18 mm. Peak negative pressure (PNP) at 1 s intervals was increased in steps of 25 kPa, starting from 50 kPa until it reached 300 kPa. PNP was measured with needle hydrophone HNR-1000 (ONDA, Sunnyvale, Canada) in the center of half-cut polysterene cuvette (CarlRoth, Germany) during full immersion into distilled degassed water bath. Acoustic responses of MBs were monitored with pulse echo broadband substitution method (GOERTZ *et al.*, 2007; ESOFFFRE *et al.*, 2013; SUN *et al.*, 2014). Applying this method in fixed path pulse transmission setup, the diffraction correction becomes less important and alignment tolerances less stringent, but the measurements are relative to the attenuation coefficient of a reference liquid (water). The computerized ultrasound pulser-receiver USBox SX (Lecoeur Electronique, Chuelles, France) was used as ultrasound monitoring system. The monitoring US transducer was spherically focused at 30 mm in water with the aperture diameter of 12 mm (model TS 12 PB 2-7 P30, Karl Deutsch Pruf- und Messgeratebau GmbH,

Wuppertal, Germany). Monitoring transducer was excited from USBox SX pulser achieving acoustic pulses at the focal spot of 20 kPa PNP, of 4.6 MHz center frequency, 0.13 µs half-maximum pulse duration and 80 Hz repetition frequency. Such short excitation pulse was chosen to enable wide-frequency-band spectral analysis. The strength of monitoring pulses was adjusted to 20 kPa PNP because such US intensity did not alter reference pulse attenuation in MB suspension during 10 s of monitoring. Thus, we assume that our monitoring system had minimal impact on MB sonodestruction. The receiver amplification was set to 38 dB, on – board filter was set to 10 MHz and the length of acquired echogram was 7000 samples (or 87 µs, or 64 mm). The -20 dB bandwidth of monitoring system was experimentally determined in 0.5–13 MHz frequencies. The diagram of reference spectra, called "S0r", is presented in Fig. 1c. The analog to digital converter was working at 12 bits amplitude resolution and taking samples at 80 MHz frequency.

The beam of monitoring transducer was fixed perpendicularly to the beam of excitation transducer. 1 ml of MB suspension was in the intersection of beams, placed in a polystyrene cuvette with 10×10 mm internal dimensions (Carl Roth GmbH+Co, Germany). The beams of the excitation and diagnostic transducers were aligned in pulse-echo mode with the use of target in the center of the experimental cuvette. The 1 mm diameter steel ball was used as a target. It was fixed in the center of the cuvette filled with agar. First the excitation transducer was fixed in the position of maximal amplitude of pulse reflected from the target (steel ball). When the excitation transducer was stably fixed, the diagnostic transducer was aligned in the same manner. The diagnostic channel was working continuously during all experiment at 80 Hz while excitation signal of preprogramed duration of 1 second were initiated manually at stepwise increased PNP. The schematic representation of the experimental setup is provided in Fig. 1. To exclude resonance distortions appearing in spectra of reference pulse, the original side walls were removed from cuvette similarly to (GOERTZ *et al.*, 2007) and covered with thin (~28 µm) US transparent mylar membrane (LORETO *et al.*, 2003). The opposite side of the cuvette was covered and sealed with 10 mm thick Plexiglas plate, which allows us to avoid reverberation distortion of reference pulse.

To assure that the monitoring US beam was perpendicular with Plexiglas plate, we found maximal amplitude of reference pulse and permanently fixed monitoring transducer before sampling of data. To acquire US signals during the experiment, pulse-echo operation mode of computerized ultrasound USBox SX pulser-receiver was used. The acquired US signals were saved on a computer hard-disc for off-line analysis.
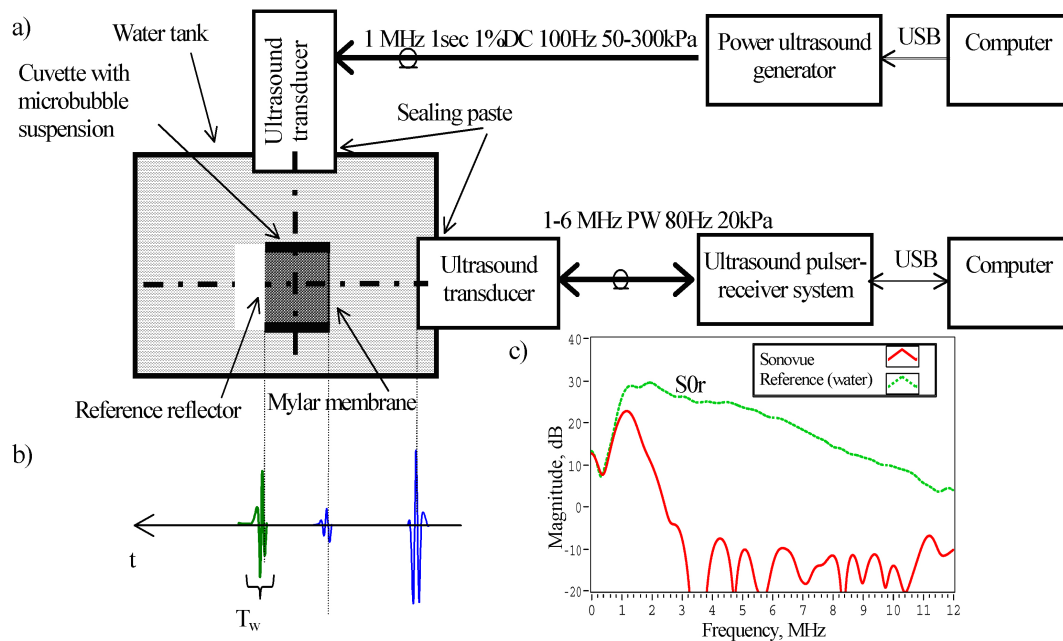
Fig. 1. An experimental setup: a) hardware setup for evaluation of acoustic response from US excited MB; b) example of echogram under investigation; c) examples of amplitude spectra of echo pulse (T_w) from reference reflector.

2.3. Attenuation analysis methods

Analysis of US recorded signals was performed off-line according to substitution method. Attenuation was analyzed during time in two aspects: 1) attenuation spectrum changes in long time-scale during whole duration MB concentration decay, 2) attenuation spectrum specific changes, in short time-scale just before and during US exposure. These two aspects of attenuation were evaluated taking different reference spectra: 1) the single reference S0r at the end of the experiment, 2) the individual references S1r – S3r just before US excitation. Beginning and ending of time window for reference spectra evaluation are indicated with arrows on a time scale in a bottom panel of Fig. 2.

The signals were read from files and analysis was started with identification of reference pulse reflected from reference reflector. Reference pulse was selected with time window (see T_w in Fig. 1b) of the Hanning shape and 3.75 µs duration. The amplitude spectra of selected pulse were calculated with fast Fourier transformation using zero padding to 16384. Logarithm of amplitude spectra was calculated and further operations were performed with logarithmic quantities. Reference pulse amplitude was found to increase during US exposure of suspension with MB. At the end of US exposure the reference pulse obtained maximal amplitude resulting from negligible attenuation in suspension as in case of pure water. An amplitude spectrum of maximal amplitude reference pulse was denoted as a reference spectrum S0r (see dotted line in Fig. 1c). The acoustic attenuation of suspension with MBs, as

a function of frequency, was determined on long time-scale by subtracting reference spectrum S0r from the spectrum during monitoring of passive and US excited MBs. Only the spectral amplitudes were subtracted. This subtraction eliminates spectral features of ultrasonic monitoring channel (including transducer and receiver with filters). Subtraction of reference spectrum compensated for non-uniform transducer frequency response. The attenuation coefficient expressed as attenuation per unit length was derived dividing result of subtraction by double width of cuvette (2 cm).

The attenuation coefficient spectrum was obtained in relation with time and PNP of excitation pulses. The variations of attenuation coefficient spectrum in time were coded in grayscale and presented as intensity chart or so called spectrogram (Fig. 2). Additionally, we analyzed the same amplitude spectra data according to the second aspect on the short time-scale. We evaluated specific and transient changes of attenuation spectrum just before and during US excitation of MB suspension when the individual reference spectra (called S0r...S3r) were used in attenuation calculation. Obtaining temporal changes of attenuation spectra of US excited MB two spectra were evaluated: 1) during 1 second before start of excitation mean reference spectra S0r...S3r was averaged; 2) during 1 second excitation the mean spectra of US excited MB S1...S3 was calculated as well. Time windows of S1...S3 and S1r...S3r estimation are indicated in a bottom panel of Fig. 2. Thus, temporal attenuations in US excited MB suspensions were obtained at increased excitation amplitudes 50, 75 and 100 kPa.
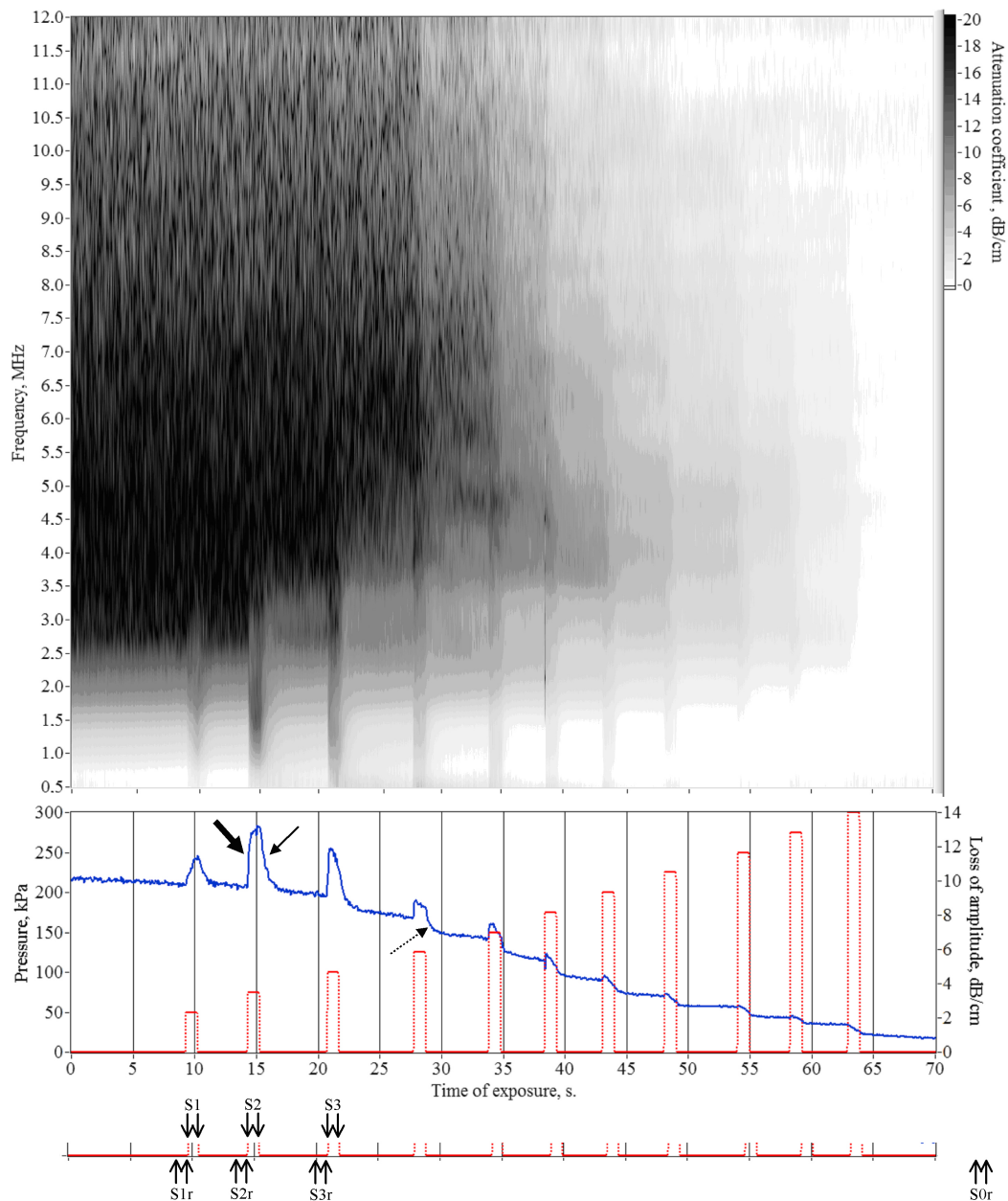
Fig. 2. The representative spectrogram of attenuation coefficient in suspension of SonoVue microbubbles (upper panel) and changes of losses of reference pulse amplitude (solid line, lower panel) obtained exposing MBs to a stepwise increased PNPs. MBs were exposed for 1 s to 1 MHz US burst signal with 1% duty cycle, 100 Hz repetition frequency. Attenuation coefficient is greyscale-coded. The On/Off waveform (dotted line) of US burst excitation is shown in the lower panel. The time window locations, where reference spectra S0r-S3r and attenuation coefficient S1-S3 were evaluated is indicated on the same time axis.

Ultrasound wave attenuation can be expressed as a ratio of two amplitudes A and A0 on a logarithmic scale $20\log_{10}(A/A0)$ per length unit [dB/cm] (SZABO, 2013). The reference pulse attenuation or loss of the amplitude of US waves propagated through the MB suspension was calculated from reference pulse in time domain. Similarly for the attenuation coefficient, the double peak value (A) was normalized to the value obtained in a cuvette with pure water (A0) and was divided by double width of the cuvette (2 cm).

3. Results and discussion

We evaluated spectra of attenuation during MB excitation with stepwise increase of PNPs. Attenuation coefficient changes were plotted in frequency and time dimensions, which allowed us to evaluate changes of attenuation spectra over the time. Typical spectrogram of attenuation coefficient at frequencies from 0.5 up to 12 MHz and time up to 70 s is shown in Fig. 2. A monotonic decrease of reference pulse amplitude loss corre-

sponding to MB excitation at different PNPs is plotted in the lower part of the figure (solid line). The amplitude loss slowly and continuously decreased over time in the absence of US excitation. A transient increase of the reference pulse amplitude loss appeared (bold arrow, Fig. 2) at the onset of the US excitation signal at 50 kPa and vanished (arrow, Fig. 2) with some delay after the end of US exposure. With some delay after the end of the first US excitation the increment disappeared and the reference pulse amplitude loss was stabilized on the slope of monotonic decrease. Further increase in PNP up to 75 kPa resulted in the maximal reference pulse amplitude loss increment and reached 3.5 dB/cm. At higher PNPs the reference pulse amplitude loss increment progressively decreased and completely disappeared at 250–275 kPa (Fig. 2). The decrease of amplitude loss at the end of US excitation signal was negligible at low PNPs, namely at 50 and 75 kPa, however, this decrease started to be substantial with further increase of PNPs (dotted arrow, Fig. 2). The decrease of attenuation coefficient was shown to reflect MB sonodestruction (Casciaro *et al.*, 2007) and makes it possible to use this parameter for estimation of MB sonodestruction kinetics (Tamosiunas *et al.*, 2012).

An increase in attenuation at low PNP values has been also reported by several research groups (Chen *et al.*, 2002; Emmer *et al.*, 2009; Casciaro *et al.*, 2007). Casciaro *et al.* (2007) found that at 50 kPa PNP attenuation was increased, while at higher PNP values attenuation was decreasing. In our case reference pulse amplitude loss increase also appeared at 50 kPa PNP, and it was observed until PNP reached 250–275 kPa, indicating that below these values our system allowed to observe additional behaviour of excited Sonovue MB. Differently from above mentioned authors, attenuation measurement in a real time showed that at low PNPs increase of the amplitude loss was transient: it appeared with the onset of US excitation and vanished with some delay after US excitation was switched off. There are several possibilities that could determine this phenomenon. Firstly, the attenuation transient increment could be caused by the transient changes in the MB diameter. Under US excitation at low PNP values MB starts to oscillate for some duration without entering sonodestruction phase. Indeed, it has been shown that due to US excitation MB can increase or decrease in size up to two times (van Wamel *et al.*, 2006). The decrease of the transient increments of attenuation and monotonic decrements of attenuation at higher PNP values was most probably related to the onset of MB sonodestruction after several oscillation cycles. Since the resonance frequency is inversely proportional to MB size, the changes in MB size as well as MB fragmentation (Postema, Schmitz, 2007) and aggregation (Dayton *et al.*, 1997) can be also reflected in differences of spectral features. Therefore alterna-

tively, the attenuation increments could arise due to fragmentation of large MBs into several smaller ones (Postema, Schmitz, 2007). Dissolution of the fragments of MBs could also lead to changes of attenuation (Bouakaz *et al.*, 1999; Postema *et al.*; 2004). When the US delivery was switched off, small but unstable MBs could coalescence and form fewer in number but larger MBs (Luan *et al.*, 2012; Chatterjee *et al.*, 2005; Krasovitski *et al.*, 2004), which also could contribute to changes in temporal attenuation increments. The third possibility of transiently increased attenuation could be due to MB aggregation and redistribution caused by US-induced radiation force (Dayton *et al.*, 1997; Tortoli *et al.*, 2000; Perelomova, Wojda, 2009). This could also partially explain prolonged duration of increase in attenuation after excitation is switched off.

Our results support the increase in MB diameter and/or formation of MB clusters that occur during MB oscillations. Indeed, the temporal increments in attenuation were mainly observed at low frequencies (1–4 MHz, see Fig. 2a). This could be attributed to appearance of aggregated clusters of MBs (Dayton *et al.*, 1997; Postema, Schmitz, 2007; Krasovitski *et al.*, 2004; Fan *et al.*, 2014). At higher spectral frequencies, although some attenuation was present, temporal changes in attenuation were negligible, showing that MB fragmentation or dissolution was minimal at low PNP. Moreover, we performed similar experiment to evaluate reference pulse amplitude loss during US excitation at 100 kPa PNP without and with MB stirring (Fig. 3). The stirring was performed using the 3×1 mm magnet bar in a cuvette with MB suspension and a magnetic stirrer. In this experiment MB mixing was switched on at 31 s and lasted till the end of the experiment. Stirring alone increased amplitude loss in 2 dB/cm, see jump of solid line at 31 s (Fig. 3). As previously, in the absence of MB stirring, we observed temporal increments in reference pulse amplitude loss during US excitation. Notably, after MB stirring was switched on we also observed temporal increments in amplitude loss. These results demonstrated that the appearance of the temporal increments in reference pulse amplitude loss was not only due to the radiation force induced non-homogeneity in the MB media or MB aggregation, but also due to MB oscillation.

In order to validate MB oscillations, we additionally performed analysis of attenuation coefficient spectra before and during MB excitation with the US at 50, 75 and 100 kPa PNP. An attenuation coefficient spectrum, during the excitation, when MBs were excited, is provided in Fig. 4. Transient increase of attenuation coefficient spectra was maximal at 1.5 MHz frequency which is consistent with other published studies (Tang, Eckersley, 2007; Piron *et al.*, 2012). Taking into account that the frequency, at which the pressure amplitude loss of the US wave is the largest, can
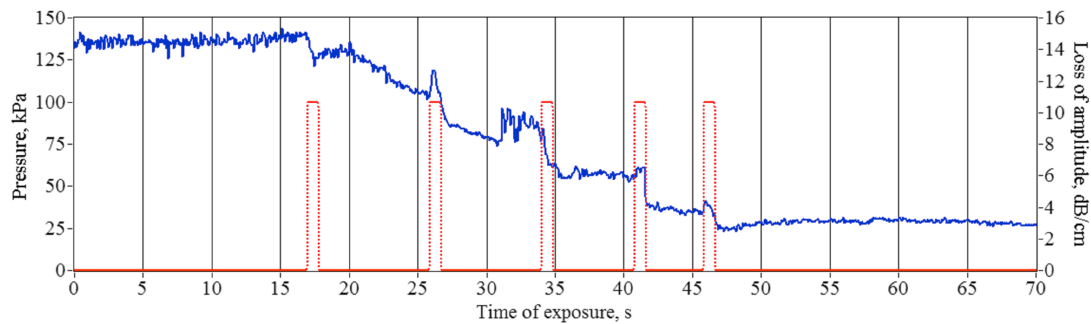
Fig. 3. The representative diagram of changes of losses of reference pulse amplitude (solid line) in suspension of SonoVue microbubbles without and with MB stirring. The MB stirring started at 31 s and lasted till the end of the experiment. 100 kPa PNP, 1 MHz US signal with 1% duty cycle, 100 Hz repetition frequency and 1 s total duration was used. The On/Off waveform of US burst excitation (dotted line) is shown at the same time axis.
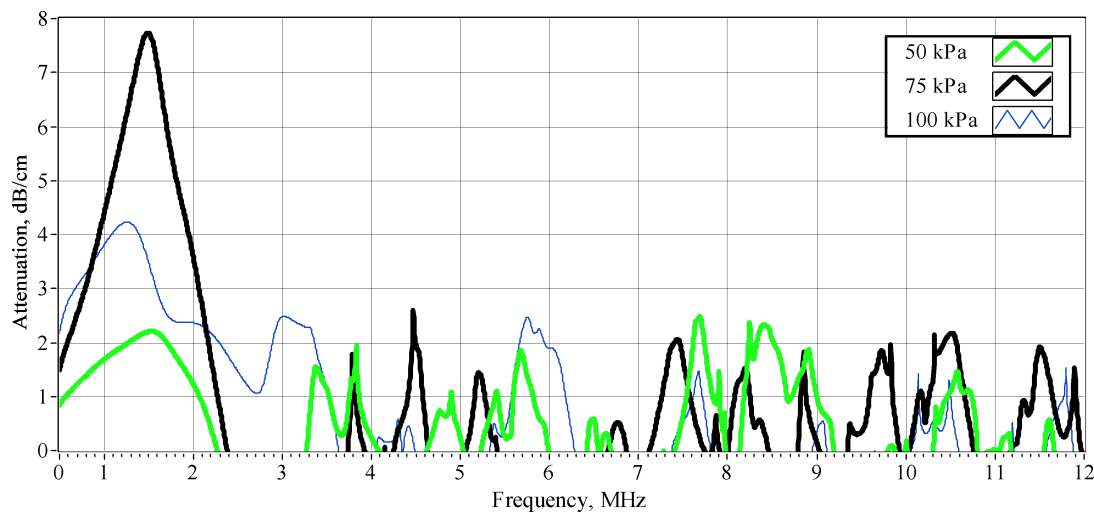

Fig. 4. Resonance frequency and ultraharmonics of excited SonoVue MBs attenuation spectra (averaged $n = 10$), when low PNP was applied. The attenuation spectra were evaluated during US application (50–75–100 kPa PNP, 1 MHz, 1% duty cycle, 100 Hz PRF and 1 s total exposure duration) as a reference using averaged spectra before onset of the application.

be identified as a MB resonance frequency (DICKER *et al.*, 2013), we believe that we observe the resonance frequency of excited SonoVue MB. The particular features of resonance in attenuation coefficient become evident only after comparison of unexcited and excited spectra. In support to this assumption, Tang and Eckersley in 2007 showed that for Sonovue MB attenuation is highly dependent on the insonation pressure around 1.5 MHz, suggesting this is the resonance frequency of microbubble population. Also, EMMER *et al.* (2009) measured frequency dependence of attenuation by BR14 (Bracco, Milan, Italy) MB. They obtained maximum attenuation at a frequency of 1.6 MHz and stated that this frequency is an indication of the resonance frequency of native BR14 suspensions. Furthermore, what was not observed in similar attenuation measurements or not published yet, we observe multiple peaks in attenuation coefficient spectra. At 75 kPa PNP, besides the resonance frequency, we ob-

served peaks at 4.5 and 7.5 MHz (see solid line in Fig. 4), which corresponded to 3 and 5 harmonic of resonance frequency.

Similar nonlinear response was observed for SonoVue, Optison, Definity and other laboratory made bubbles (AMARARENE *et al.*, 2001; GOERTZ *et al.*, 2005; EMMER *et al.*, 2009; STOLZ *et al.*, 2002). This behaviour was proposed to be related to changes in MB diameter during US excitation (GOERTZ *et al.*, 2006; BIAGI *et al.*, 2005). The increased attenuation coefficient at certain frequencies can be related to increased scattering by excited MB in suspension. These pilot observations inspired improvement of experimental system. Our further research of temporal attenuation increments in suspension of excited MB is aimed to synchronize monitoring at higher temporal resolution.

In conclusion, we propose a new method to monitor MB acoustic response. Fast measurement signals

allowed examination of attenuation in suspension with passive and excited MBs in a real time. The method allows rapid valuation of the of resonance frequency of MB, onset and kinetics of MB sonodestruction.

Acknowledgments

References

1. Amararene J., Fowlkes B., Song J., Miller D.L. (2001), *Relationships between scattered signals from ultrasonically activated contrast agents and cell membrane damage in vitro*, Ultrasonics Symposium, IEEE, **2**, 1751–1754.

2. Biagi E., Breschi L., Masotti L. (2005), *Transient subharmonic and ultraharmonic acoustic emission during dissolution of free gas bubbles*, IEEE Trans. Ultrason. Ferroelectr. Freq. Control, **52**, 6, 1048–1054.

3. Bouakaz A., Frinking P.J., de Jong N., Bom N. (1999), *Noninvasive measurement of the hydrostatic pressure in a fluid-filled cavity based on the disappearance time of micrometer-sized free gas bubbles*, Ultrasound Med. Biol., **25**, 9, 1407–1415.

4. Burns P.N., Becher H. (2000), *Contrast agents for echocardiography: Principles and instrumentation*, [in:] Handbook of contrast echocardiography: Left ventricular function and myocardial perfusion, Becher H., Burns P.N. [Eds.], pp. 2–44, Springer, Heidelberg.

5. Casciaro S., Palmizio E.R., Conversano F., Demitri C., Distante A. (2007), *Experimental investigations of nonlinearities and destruction mechanisms of an experimental phospholipid-based ultrasound contrast agent*, Invest. Radiol., **42**, 2, 95–104.

6. Chatterjee D., Jain P., Sarkar K. (2005), *Ultrasound-mediated destruction of contrast microbubbles used for medical imaging and drug delivery*, Phys. Fluids, **17**, 100603-1-8.

7. Chen Q., Zagzebski J., Wilson T., Stiles T. (2002), *Pressure-dependent attenuation in ultrasound contrast agents*, Ultrasound Med. Biol., **28**, 8, 1041–1051.

8. Dayton P.A., Morgan K.E., Klibanov A.L.S., Brandenburger G., Nightingale K.R., Ferrara K.W. (1997), *A preliminary evaluation of the effects of primary and secondary radiation forces on acoustic contrast agents*, IEEE Trans. Ultrason. Ferroelectr. Freq. Control, **44**, 1264–1277.

9. de Jong N., Hoff L., Skotland T., Bom N. (1992), *Absorption and scatter of encapsulated gas filled microspheres: theoretical considerations and some measurements*, Ultrasonics, **30**, 2, 95–103.

10. Dicker S., Mleczko M., Siepmann M., Wallace N., Sunny Y., Bawiec C.R., Schmitz G., Lewin P., Wrenn S.P. (2013), *Influence of shell composition on the resonance frequency of microbubble contrast agents*, Ultrasound Med. Biol., **39**, 7, 1292–1302.

11. Emmer M., Vos H. J., Goertz D.E., van Wamel A., Versluis M., de Jong N. (2009), *Pressure-dependent attenuation and scattering of phospholipid-coated microbubbles at low acoustic pressures*, Ultrasound Med. Biol., **35**, 1, 102–111.

12. Escoffre J.M., Novell A., Piron J., Zeghimi A., Doinikov A., Bouakaz A. (2013), *Microbubble Attenuation and Destruction: Are They Involved in Sonoporation Efficiency?*, IEEE Trans. Ultrason. Ferroelectr. Freq. Control, **60**, 1,46–52.

13. Fan Z., Chen D., Deng C.X. (2014), *Characterization of the dynamic activities of a population of microbubbles driven by pulsed ultrasound exposure in sonoporation*, Ultrasound Med. Biol., **40**, 6, 1260–1272.

14. Goertz D.E., Cherin E., Needles A., Karshafian R., Brown A. S., Burns P.N., Foster F.S. (2005), *High Frequency Nonlinear B-Scan Imaging of Microbubble Contrast Agents*, IEEE Trans. Ultrason. Ferroelectr. Freq. Control, **52**, 1, 65–79.

15. Goertz D.E., de Jong N., van der Steen A.F. (2007), *Attenuation and size distribution measurements of Definity and manipulated Definity populations*, Ultrasound Med. Biol., **33**, 9, 1376–1388.

16. Goertz D.E., Frijlink M.E., de Jong N., van der Steen A.F. (2006), *High frequency nonlinear scattering from a micrometer to submicrometer sized lipid encapsulated contrast agent*, Ultrasound Med. Biol., **32**, 4, 569–677.

17. Krasovitski B., Kimmel E., Sapunar M., Adam D. (2004), *Ultrasound attenuation by encapsulated microbubbles: time and pressure effects*, Ultrasound Med. Biol., **30**, 6, 793–802.

18. Lamanauskas N., Novell A., Escoffre J.M., Venslauskas M., Satkauskas S., Bouakaz A. (2013), *Bleomycin delivery into cancer cells in vitro with ultrasound and SonoVue® or BR14® microbubbles*, J. Drug Target, **21**, 4, 407–414.

19. Loreto B., Feril Jr., Takashi K., Qing-Li Z., Ryohei O., Katsuro T., Nobuki K., Shinichi F., Shinobu N. (2003), *Enhancement of ultrasound-induced apoptosis and cell lysis by echo-contrast agents*, Ultrasound Med. and Biol., **29**, 2, 331–337.

20. Luan Y., Faez T., Gelderblom E., Skachkov I., Geers B., Lentacker I., van der Steen T., Versluis M., de Jong N. (2012), *Acoustical properties of individual liposome-loaded microbubbles*, Ultrasound Med. Biol., **38**, 12, 2174–2185.

21. Perelomova A., Wojda P. (2009), *Acoustic Streaming Caused by Some Types of Aperiodic Sound. Buildup of Acoustic Streaming*, Archives of Acoustics, **34**, 4, 625–639.

22. Piron J., Escoffre J.M., Kaddur K., Novell A., Bouakaz A. (2012), *Enhanced gene transfection using ultrasound and Vevo Micromarcer microbubbles*, Ult. Sym., **10**, 1109.

23. Postema M., Bouakaz A., de Jong N. (2004), *Noninvasive microbubble-based pressure measurements: a simulation study*, Ultrasonics, **42**, 1–9, 759–762.

24. POSTEMA M., SCHMITZ G. (2007), *Ultrasonic bubbles in medicine: influence of the shell*, Ultrasonics Sonochemistry, **14**, 4, 438–444.

25. SARKAR K., SHI W.T., CHATTERJEE D., FORSBERG F. (2005), *Characterization of ultrasound contrast microbubbles using in vitro experiments and viscous and viscoelastic interface models for encapsulation*, J. Acoust. Soc. Am., **118**, 1, 539–550.

26. STOLZ E., ALLENDÖRFER J., JAUSS M., TRAUPE H., KAPS M. (2002), *Sonographic harmonic grey scale imaging of brain perfusion: scope of a new method demonstrated in selected cases*, Ultraschall. Med., **23**, 5, 320–324.

27. SUN C., SBOROS V., BUTLER M.B., MORAN C.M. (2014), *In vitro acoustic characterization of three phospholipid ultrasound contrast agents from 12 to 43 MHz*, Ultrasound Med, Biol., **40**, 3, 541–550.

28. SZABO T.L. (2004), *Diagnostic Ultrasound Imaging: Inside Out*, Elsevier Academic Press, London, p. 83.

29. TAMOSIUNAS M., JURKONIS R., MIR L.M., LUKOSEVICIUS A., VENSLAUSKAS M.S., SATKAUSKAS S. (2012), *Adjustment of ultrasound exposure duration to microbubble sonodestruction kinetics for optimal cell sonoporation in vitro*, Technol. Cancer Res. Treat., **11**, 4, 375–387.

30. TANG M.X., ECKERSLEY R.J. (2007), *Frequency and pressure dependent attenuation and scattering by microbubbles*, Ultrasound Med. Biol., **33**, 1, 164–168.

31. TANG M.X., ECKERSLEY R.J., NOBLE J.A. (2005), *Pressure-dependent attenuation with microbubbles at low mechanical index*, Ultrasound Med. Biol., **31**, 3, 377–384.

32. TANG M.-X., MULVANA H., GAUTHIER T., LIM A.K.P., COSGROVE D.O., ECKERSLEY R.J., STRIDE E. (2011), *Quantitative contrast-enhanced ultrasound imaging: a review of sources of variability*, Interface Focus, **1**, 520–539.

33. TORTOLI P., PRATESI M., MICHELASSI V. (2000), *Doppler spectra from contrast agents crossing an ultrasound field*, IEEE Trans. Ultrason. Ferroelectr. Freq. Control, **47**, 3, 716–726.

34. VAN WAMEL A., KOOIMAN K., HARTEVELD M., EMMER M., TEN CATE F.J., VERSLUIS M., DE JONG N. (2006), *Vibrating microbubbles poking individual cells: drug transfer into cells via sonoporation*, J. Control Release., **112**, 2, 149–155.